

The mechanism of the polarization dependence of the optical transmission in subwavelength metal hole arrays

Qian Zhao¹, Chao Li¹, Yun-Song Zhou^{1,†}, Huai-Yu Wang^{2,‡}

¹ *Center of Theoretical Physics, Department of Physics,
Capital Normal University. Beijing 100048, China and*

² *Department of Physics, Tsinghua University, Beijing 100084, China*

(Dated: November 22, 2021)

Abstract

We investigate the mechanism of extraordinary optical transmission in subwavelength metal hole arrays. Experimental results for the arrays consisting of square or rectangle holes are well explained about the dependence of transmission strength on the polarization direction of the incident light. This polarization dependence occurs in each single-hole. For a hole array, there is in addition an interplay between the adjacent holes which is caused by the transverse magnetic field of surface plasmon polariton on the metal film surfaces. Based on the detailed study of a single-hole and two-hole structures, a simple method to calculate the total transmissivity of hole arrays is proposed.

PACS numbers: 78.68.+m, 78.20.-e, 42.25.Hz, 78.35.+c, 42.97.-e

1. Introduction

The extraordinary optical transmission (EOT) [1,2] in a subwavelength metal hole array is an interesting topic[3-12] because its mechanism is still in exploring and it shows abundant features. One of the features is that the transmissivity may depend on the polarization direction of the incident light. Disclosing clearly the reason behind the dependence is helpful to adjusting the EOT strength, as well as to applying the EOT in optical devices. Lots of experiments have been done for light in visible [3-7,13-17], infrared [8-10], and terahertz [11,12,18,19] regions to observe the dependence of EOT on polarization of the incident light. We here sort both the arrays and holes into three kinds, respectively, as summarized in Table 1. It is seen from Table 1 that among nine structures, five have been fabricated to observe the dependence of the EOT on the light polarization. In the second column, a square lattice consisting of rectangle holes shows polarization dependence while that consisting of square holes does not. In order to disclose the reason behind the discrepancy, a theoretical investigation is desirable.

Table 1. The experimental results that whether EOT is dependent on the polarization of the incident light or not. The names in parentheses are used in Sec.5.

	Square lattice	Rectangle lattice	Single hole
Square hole	Independent[11,16] (S-S array)	Unreported (S-R array)	Unreported
Rectangle hole	Dependent[11,15-19] (R-S array)	Unreported (R-R array)	Dependent[14,15]
Circle hole	Independent[3-5,13]	Dependent[5-7,11,13]	Unreported

A lot of theoretical works about EOT in hole arrays have been reported[20], they are mainly focused on the mechanism or factors that cause in or influence EOT in hole arrays. A few of them investigate the polarization dependence of EOT in hole array or single hole [21-25] . Garcia *et al.* [21] carried out a rigorous solution of Maxwell's equations so as to obtain the transmission of circle holes perforated in a thin perfect-conductor screen for s and p polarization. Gordon *et al*[22] explained the polarization dependence in array of elliptic holes in terms of the interaction between SPP and the periodic lattice grating. Notwithstanding the approaches done, the systematical investigation about the polarization dependence is still desirable.

In our opinion, when considering the EOT in an array consisting of holes (or slits), there are basically the single-hole (slit) effect and the inter-hole (slit) effect [26]. The former reflects the transmissivity behavior of the light going through single subwavelength holes, and the latter means the possible modulation of transmissivity arising from the influence by neighboring holes. Supposing that the polarization dependence does exist, then one should know if the dependence is caused by the single-hole or inter-hole effect or both.

In this paper we investigate the mechanism of the polarization dependence of the EOT in a hole array consisting of square or rectangle holes. Based on our simulation results by finite-difference time-domain (FDTD) method [27], we reveal the mechanism of the polarization dependence and explain the experimental results. Furthermore, we find that it is possible to get a simple way to calculate the transmissivity of the hole array, which may avoid the burdensome simulation work in hole arrays.

This paper is arranged as follows. In section 2 the hole-array model is established. Before studying the EOT of the array, we study in detail the EOT of a single-hole and double-hole structures in sections 3 and 4, respectively, so as to clearly show the single-hole and double-hole effects. Then the EOT in a hole array is researched in section 5. In doing so, a simple method is proposed to calculate the transmissivity of the hole array. In section 6 the simple method proposed in Sec. 5 is applied to some arrays. It appears that the application is satisfactory. Section 7 gives our summary.

2. The array model

Our model is sketched in Fig. 1. Rectangle holes drilled on a metal film form a two-dimensional lattice, consisting of rectangle cells, in xy plane. The lengths of two sides of each hole are a and b , and the lattice constants are A and B , respectively. A linearly polarized TM wave illuminates this structure along z -direction. Before impinging the structure, the magnetic and electric components are H_0 and E_0 , respectively. In simulation we always use

$$E_0 = H_0 = 0.31. \quad (1)$$

The angle between y axis and E_0 direction is θ . Hereafter the light is termed as ”

θ -polarized". From Fig. 1 the x and y components of electric and magnetic fields are

$$\left. \begin{aligned} E_{0x} &= E_0 \sin \theta \\ E_{0y} &= E_0 \cos \theta \end{aligned} \right\}, \quad (2a)$$

$$\left. \begin{aligned} H_{0x} &= -H_0 \cos \theta \\ H_{0y} &= H_0 \sin \theta \end{aligned} \right\}. \quad (2b)$$

The metal film with thickness $h = 2\mu m$ is made of silver. The incident wave length is $\lambda_0 = 0.6\mu m$. The dielectric constant of silver vs. wavelength can be expressed as $\epsilon_{Ag} = 3.57 - 54.33\lambda_0^2 + i(-0.083\lambda_0 + 0.921\lambda_0^3)[26,28]$. Thus, as $\lambda_0 = 0.6\mu m, \epsilon_{Ag} = -15.989 + i0.1491$.

When light goes through the array, the surface plasmon polariton (SPP) will be excited in every hole and the metal surfaces. Since it is a TM wave, after entering the holes, the electric field may have a z -component, while the magnetic field does not. In each hole there is a strong power, denoted as P . In simulation, this power value P is measured by a monitor M placed at the exit of the hole labeled by "0". If the whole structure is removed, the power measured by this monitor at the same place is denoted as P_0 [20,22]. The transmissivity of this hole is defined as $T = P/P_0$.

Our simulated result is the transmissivity T . Since T is simply linearly proportional to Poynting vector S , we will analyze the construction of S to explain the expression of T obtained by simulation.

Since the array consists of holes, the light behavior in any one hole and the correlation between holes are essential in realizing the light behavior when light going through the whole array. Therefore, before studying the whole array, we explore the light behavior when it goes through only one hole and a two-hole structure.

3. The single-hole structures

Letting all the holes in the array except the one labeled by "0" in Fig. 1 be closed, we set up a one-hole structure. We will study the cases where the hole is a square and a rectangle, respectively.

Suppose that the amplitudes of the components of electromagnetic field in the hole are E_x^{hole} , E_y^{hole} , H_x^{hole} and H_y^{hole} , respectively. It is found from the simulated results that these

amplitudes as functions of angle θ can be expressed by following way:

$$\left. \begin{aligned} E_x^{hole} &= E_{0,x}^{hole} \sin \theta \\ E_y^{hole} &= E_{0,y}^{hole} \cos \theta \end{aligned} \right\}, \quad (3a)$$

$$\left. \begin{aligned} H_x^{hole} &= -H_{0,x}^{hole} \cos \theta \\ H_y^{hole} &= H_{0,y}^{hole} \sin \theta \end{aligned} \right\}. \quad (3b)$$

Equation (3) tells us that, when studying a single rectangle hole, one merely needs to measure the field components at an arbitrary polarization angle θ so as to get the amplitudes $E_{0,x}^{hole}$, $E_{0,y}^{hole}$, $H_{0,x}^{hole}$ and $H_{0,y}^{hole}$ in the hole by Eq.(3). Then the field components at any other angle θ can be easily calculated in terms of Eq.(3).

It is noticed that the angular dependence of the left hand side of Eq. (3) is identical to that of Eq. (2). Based on this fact, we introduce a concept of SPP polarization excitation ratios (PERs) of each field component: the ratio of amplitude of field component in the hole to that in vacuum. They are denoted by η_{Ex} , η_{Ey} , η_{Hx} , and η_{Hy} respectively, and expressed as follows:

$$\left. \begin{aligned} \eta_{Ex} &= E_x^{hole} / E_{0x} = E_{0,x}^{hole} / E_0 \\ \eta_{Ey} &= E_y^{hole} / E_{0y} = E_{0,y}^{hole} / E_0 \end{aligned} \right\}, \quad (4a)$$

$$\left. \begin{aligned} \eta_{Hx} &= H_x^{hole} / H_{0x} = H_{0,x}^{hole} / H_0 \\ \eta_{Hy} &= H_y^{hole} / H_{0y} = H_{0,y}^{hole} / H_0 \end{aligned} \right\}. \quad (4b)$$

For example, η_{Ex} is called the x -component SPP electric field PER. Since the SPP electromagnetic field PERs are independent of angle, they are used to describe the basic property of the hole.

As long as the field amplitudes in the hole are measured, the total curve of the transmission power or transmissivity can be obtained. To explain the transmissivity, one needs to calculate Poynting vector $\mathbf{S} = \mathbf{E} \times \mathbf{H}$.

In the hole, the averaged value in a time period of z -component of Poynting vector is

$$S_z^{hole} = (E_x^{hole} H_y^{hole} - E_y^{hole} H_x^{hole})/2, \quad (5a)$$

$$S_z^{hole} = (E_{0,x}^{hole} H_{0,y}^{hole} \sin^2 \theta + E_{0,y}^{hole} H_{0,x}^{hole} \cos^2 \theta)/2. \quad (5b)$$

Let us first investigate the case of a square hole. The parameters are taken as $a = b = 0.2\mu m$. The power measured in this hole is denoted as P^{hole} and the transmissivity of the

hole is defined as $T_0 = P^{hole}/P_0$. The simulated transmissivity values are plotted in Fig. 2 by crosses. Figure 2 shows that as θ angle changes, T_0 varies between 19.31 and 19.38. Since the variation scope is within calculation error, the transmissivity is regarded as unchanged, i.e., it is independent of the polarization.

The calculated amplitude values of x and y components of electromagnetic fields of SPP in the hole are presented in Fig. 2 by square and circle symbols. The results are easily fitted by curves in terms of Eq. (3). Here, we have

$$E_{0,x}^{hole} = E_{0,y}^{hole} = 1.88, \quad (6a)$$

$$H_{0,x}^{hole} = H_{0,y}^{hole} = 1.21. \quad (6b)$$

Equation 6 exhibits two features. One is that the dimensions of the field component amplitudes $E_{0,x}^{hole}$, $E_{0,y}^{hole}$, $H_{0,x}^{hole}$ and $H_{0,y}^{hole}$ in the hole are larger than those outside the hole E_{0x} , E_{0y} , H_{0x} and H_{0y} respectively. This reflects the EOT character, i.e., the transmissivity T_0 is greater than 1, as a subwavelength hole should have. The other is that the electromagnetic fields in a square hole behave as isotropic. This is an important feature of a square hole, which has been discovered by experiments, as shown in Table. 1. Later we will see that for a rectangular holes it is not so.

For a square hole, substituting Eq. (6) into Eq. (5b), one obtains

$$S_z^{hole} = E_{0,x}^{hole} H_{0,y}^{hole} / 2 = E_{0,y}^{hole} H_{0,x}^{hole} / 2, \quad (7)$$

Here S_z^{hole} is independent of angle θ , which is the reason why the transmissivity T_0 is independent of angle θ as shown in Fig.2.

Equation (6) leads to

$$\left. \begin{aligned} \eta_{Ex} &= \eta_{Ey} \\ \eta_{Hx} &= \eta_{Hy} \end{aligned} \right\} \quad (8)$$

In other words, along the two sides of the square hole, the SPP PERs are equal. Equation (8) is the physical reason that the transmission power is independent of the polarization direction in a square hole.

Equation (8) manifests the $\pi/2$ rotation symmetry of a square hole. It is probably that if the $\pi/2$ rotation symmetry is broken, Eq. (8) will not be valid. Consequently the transmission power should change with the polarization angle.

Next we investigate the case of a rectangular hole. Experiments showed the polarization dependence of transmission in rectangular hole, see Table 1. Let us see our simulated results.

The simulation results of a rectangle hole are plotted in Fig. 3 where the two sides of the hole are $a = 0.2\mu m$ and $b = 0.1\mu m$, respectively. The crosses in Fig. 3(a) show the transmissivity T_0 . It changes with the polarization angle. The symbols in Fig. 3(b) denote the field amplitudes in the hole, which can be fitted with Eq. (3) but $E_{0,x}^{hole} = 0.69 \times 10^{-2}$, $E_{0,y}^{hole} = 2.89$, $H_{0,x}^{hole} = 1.21$, and $H_{0,y}^{hole} = 0.53 \times 10^{-2}$. With these data we obtained: $\eta_{Ex} = 0.022$, $\eta_{Ey} = 9.32$, $\eta_{Hx} = 3.90$, and $\eta_{Hy} = 0.017$. That is to say,

$$\left. \begin{array}{l} \eta_{Ex} \neq \eta_{Ey} \\ \eta_{Hx} \neq \eta_{Hy} \end{array} \right\} \quad (9)$$

The SPP PERs in x and y directions for either electric or magnetic field differs from each other. This feature is different from that of a square hole. In each direction, when the electric field is strong, then the magnetic field is weak, or vice versa.

The above discussions demonstrate that the SPP polarization excitation ratios are the key roles to exhibit the properties of the transmission with the polarization angle.

As has been mentioned above, one can choose an arbitrary polarization angle θ to get the amplitudes $E_{0,x}^{hole}$, $E_{0,y}^{hole}$, $H_{0,x}^{hole}$ and $H_{0,y}^{hole}$. In this way, one saves a lot of time and workload to avoid measuring the whole angle region as shown by solid and open symbols in Figs. 2 and 3.

Since for a square hole, the SPP PERs in two axis directions are the same, while for a rectangle one it is not, when changing the ratio b/a , the SPP PERs should vary. We keep $a = 0.2\mu m$, and change b from 0.1 to $0.3\mu m$. The simulated SPP PERs are displayed in Fig. 4 by symbols. The lines in Fig. 4 are just for guiding eyes. When the ratio b/a is small, say for $b = 0.1\mu m$, one of η_x and η_y is negligible compared to another. It seems that in this case the field components E_x^{hole} and H_y^{hole} are totally depressed. This implies that, the SPP wave is mainly polarized with the magnetic field along the longer side of the rectangle hole. In other word, with respect to the polarization properties, the rectangle hole is somehow equivalent to a slit when the ratio b/a of the hole is small. For convenience we refer to this kind of hole as slit-hole. The character of a slit-hole is that the electric or magnetic field component along one side direction is negligible compared to the other side. According to our simulation results, there exists a critical size for b beyond which the

PERs η_x and η_y are comparable to each other. For instance, when $a = 0.2\mu m$, it is found from Fig. 4 that the critical size for b is $b_c = 0.18\mu m$. When $b > b_c$, the corresponding SPP PERs rise suddenly so the character of a slit-hole disappears. In other words, the SPP mode of electric field in x direction begins to excite. As the size of b approaches that of a , η_x and η_y become closer. At $b = 0.2\mu m$, the square hole, the two solid lines meet at the value $\eta_{Ex} = \eta_{Ey} = 6.06$, and the two dashed lines meet at the value $\eta_{Hx} = \eta_{Hy} = 3.89$.

4. The double-hole structures

Now we turn to investigate the inter-hole effect. For this purpose we set up a two-hole structure by closing all the holes in the array except the two labeled by "0" and "1", hereafter referred to as 0-1 structure.

Before starting the investigation of the two-hole structure, let us briefly retrospect the EOT of a double-slit structure[20]. The SPP wave excited in one slit will interfere with that coming from the other slit. The interference varies with the inter-slit distance D . This interference is the so-called inter-slit effect. As a consequence, the total power passing through the structure oscillates with the inter-slit distance D . Each peak of the power curve corresponds to the in phase interference between the two slits.

A double-hole structure resembles a double-slit structure in that there is an interference between SPPs excited in the two holes as the SPP waves travel along the metal film surfaces, and the interference varies with the inter-hole distance. Therefore, at appropriate inter-hole distances, the interference will generate largest transmission power. In simulation, we find that one of such distances is $A = 0.4\mu m$ when $a \times b = 0.2 \times 0.2\mu m^2$ and the polarization of the incident wave is $\theta = 90^\circ$.

The transmissivity measured in this structure is denoted as T_{01} . When fixing $A = 0.4\mu m$, the variation of T_{01} as a function of the polarization angle θ is displayed by the solid circles in Fig. 5(a). The data are well fitted with the equations

$$T_{01}(\theta) = T_0 + \Delta T_{01}(\theta), \quad (10)$$

where

$$\Delta T_{01}(\theta) = 6.64 \sin^2 \theta, \quad (11)$$

and $T_0 = 19.36$. It should be noticed that T_0 is just the transmissivity of single square hole structure, see Fig. 2. Equation (10) clearly demonstrates that the total transmissivity

comprise two parts coming from the single hole and inter-hole effects, respectively. The contribution from the inter-hole effect on the transmissivity is expressed by Eq. (11). When $\theta = 0$, the inter-hole effect vanishes.

Here we intend to disclose which factors the coefficient 6.64 of the interference term involves. To do so we analyze the behaviors of the SPPs traveling from one hole to the other along x direction. That is to say, we should evaluate the Poynting vector S_x^{SPP} between the two holes. For this purpose we choose the mid-point between the centers of the two holes on the exit surface of the film as an observation point to measure S_x^{SPP} . Now we close the hole "1". Thus the system degenerates to a single-hole structure. In this case the SPPs at the observation point comes from the open hole. The observed S_x^{SPP} reads $S_x^{SPP} = E_y^{SPP} H_z^{SPP} - E_z^{SPP} H_y^{SPP}$. Our simulated results reveals that the absolute values of E_y^{SPP} and H_z^{SPP} are negligible compared to E_z^{SPP} and H_y^{SPP} . Thus we have $S_x^{SPP} = -E_z^{SPP} H_y^{SPP}$. Consequently, in the following, we merely take into account the contribution of E_z^{SPP} and H_y^{SPP} , omitting those of E_y^{SPP} and H_z^{SPP} . The simulated amplitudes of E_z^{SPP} and H_y^{SPP} at the observation point are displayed in Fig. 5(b) by solid and open circles, respectively. The solid curves in Fig.5(b) are plotted with

$$\left. \begin{aligned} E_z^{SPP} &= E_{0z}^{SPP} \sin \theta \\ H_y^{SPP} &= H_{0y}^{SPP} \sin \theta \end{aligned} \right\} \quad (12)$$

where $E_{0z}^{SPP} = 1.12$ and $H_{0y}^{SPP} = 0.82$. Comparing Eqs. (12) and (3), we find that the ratio $H_y^{hole}/H_y^{SPP} = H_{0y}^{hole}/H_{0y}^{SPP}$ is independent of angle θ , so we define this ratio as γ_{01} :

$$\gamma_{01} = \begin{cases} H_y^{SPP}/H_y^{hole} = H_{0y}^{SPP}/H_{0y}^{hole}, & \text{when } H_{0y}^{hole} \neq 0 \\ 0, & \text{when } H_{0y}^{hole} = 0 \end{cases} \quad (13)$$

This ratio is regarded as the conversion of the transverse magnetic field on surface excited by the magnetic field in the hole. It is determined by the geometry and physical parameters of the single-hole structure. The subscript "01" in γ_{01} means the SPP traveling from holes 0 to 1. In the present case, $\gamma_{01} = 0.82/1.21 = 0.68$. When $H_{0y}^{hole} = 0$, the H_y^{SPP} can not be excited, so we define $\gamma_{01} = 0$. In this case the inter-hole effect vanishes.

Now we are ready to disclose which factors the coefficient of $\sin^2 \theta$ term in Eq. (11) comprises. Let both holes in the structure open. The SPP wave from hole 0 will arrive at hole 1, it will interfere with the SPP excited in hole 1. The same process will also occur at

hole 0. In this case the total magnetic field at the exit of hole "0" includes two parts: One is H_y^{hole} contributed from "0" itself as an isolated hole, and the other is H_y^{SPP} contributed from "1". Thus the y-component of magnetic field becomes $H_y^{hole} + H_y^{SPP}$. Consequently, the Poynting vector in z -direction is

$$S_{01,z}^{hole} = E_x^{hole}(H_y^{hole} + H_y^{SPP}) - E_y^{hole} H_x^{hole} = S_z^{hole} + E_x^{hole} H_y^{SPP}, \quad (14)$$

Here S_z^{hole} is just Eq. (5a), the Poynting vector without the contribution of H_y^{SPP} . Substituting Eqs. (3), (12), and (13) into Eqs. (14) we get

$$S_{01,z}^{hole} = S_z^{hole} + \Delta S_{01,z}^{hole}, \quad (15a)$$

where

$$\Delta S_{01,z}^{hole} = 2S_{01,z}^{hole} \gamma_{01} \sin^2 \theta, \quad (15b)$$

The Poynting vector of the 0-1 structure $S_{01,z}^{hole}$ comprises two parts: a term of a single-hole structure and a term reflecting inter-hole effect between the two holes. The latter in turn is related to $S_{01,z}^{hole}$ its self. Therefore, although an angle factor $\sin^2 \theta$ is separated, the coefficient of $\sin^2 \theta$ in Eq. (15b) should generally still contain functions of angle θ . Equation (15) is linearly proportional to Eq. (10). Therefore, we can reasonably rewrite Eq. (11) in the following form:

$$\Delta T_{01}(\theta) = T_{01}(\theta) C_{01}(\theta) \sin^2 \theta, \quad (16)$$

$C_{01}(\theta)$ is the coupling coefficient that reveals the strength of inter-hole effect generated by total transmission power. Combining Eqs. (10) and (16) one achieves

$$T_{01}(\theta) = T_0 + T_{01}(\theta) C_{01}(\theta) \sin^2 \theta, \quad (17)$$

We emphasize that Eq. (17) is applicable to the double-hole structure consisting of identical rectangle holes.

In the case of square holes, we have, from Eq. (11), $T_{01}(\theta) C_{01}(\theta) = 6.64$. Thus the two expression of the two factors $T_{01}(\theta)$ and $C_{01}(\theta)$ are easily solved.

$$C_{01}(\theta) = 6.64 / (T_0 + 6.64 \sin^2 \theta), \quad (18)$$

and

$$T_{01}(\theta) = T_0 / [1 - C_{01}(\theta) \sin^2 \theta]. \quad (19)$$

Please note that since $T_0 = 19.36$, much larger than the term $6.64 \sin^2 \theta C_{01}(\theta)$ in Eq. (18) is approximately a constant. Indeed, if we select $\theta = \pi/2$, then $C_{01}(\theta) = 0.255$, and the calculated $T_{01}(\theta)$ is plotted in Fig. 5(a) by dashed line. Apparently, this is a quite good approximation.

It is worthy to point out that the inter-hole effect involves the contributions from SPP waves of both surfaces of the metal film. Equations (10), (17), and (19) have included the contribution from both surfaces.

When the nearest neighbor (nn) hole is farther and at another azimuth angle, the interference between the two holes will vary. As an example to demonstrate this, we choose the two holes labeled by "0" and "5" in the array depicted in Fig 1, while other holes are closed, to discuss the next nearest neighbor (nnn) inter-hole effect. The array constants are $A = B = 0.4\mu m$ and $a \times b = 0.2 \times 0.2\mu m^2$. The simulated transmissivity as a function of the polarization angle are plotted in Fig. 6 by solid points. The data are well fitted by solid curve in terms of following expressions:

$$T_{05} = T_0 + \Delta T_{05}, \quad (20)$$

$$\Delta T_{05} = T_{05} C_{05}(\theta) \sin^2(\theta + 45^\circ), \quad (21)$$

and

$$C_{05}(\theta) = -2.55/[T_0 - 2.55 \sin^2(\theta + 45^\circ)]. \quad (22)$$

Compared to the 0-1 structure, the 0-5 structure shows differentia in two ways. One is that the phase shift comes from the fact that the hole "5" is located at azimuth angle 45° . Correspondingly, there is the same phase shift in H_y^{SPP} compared to Eq. (12): $H_y^{SPP} = H_{0y}^{SPP} \sin(\theta + 45^\circ)$. Therefore when $\theta = 135^\circ$, there will be no propagation of H_y^{SPP} between the holes "0" and "5", i.e., the inter-hole effect vanishes at this angle. Indeed, from Eq. (21) the interference term is zero at this angle. The other is that the figure -2.55 in Eq. (22) is in the place of 6.64 in Eq. (18).

The discussion about the interference in the two-hole structures above only concerns the azimuth. Another factor affecting the interference is the distance between the two holes. Let the distance between the two holes be r . Then the transmissivity oscillates with r . This oscillation is embodied in the value of C . Our simulation results show that for present square lattice of $A = B = 0.4\mu m$, as $r = A$, $T_{01}(\theta)C_{01}(\theta) = 6.64$, which just corresponds to the

interference in phase; and when $r = \sqrt{2}A$, this distance makes the interference out of phase so that the transmission is suppressed, thus $T_{05}C_{05}(\theta) = -2.55$ is minus. From Eq. (21) we see that as $\theta = 45^\circ$ the inter-hole effect term is maximum, so that the transmissivity curve in Fig. 6 shows a valley.

We have mentioned that in the 0-1 structure, calculated $T_{01}(\theta)$ using a constant $C(\theta) = 0.255$ approximates the exact results quite well, as shown in Fig. 5. Here we again set a constant $C(\theta) = -0.152$ to compute $T_{05}(\theta)$ and the results are plotted in Fig. 6 by dashed line, which is almost identical to the solid line.

5. The hole arrays

To simulate the transmission of a hole array is quite difficult for a very large memory size is needed. However, the discussion about the two-hole structures in Sec. 4 prompts us that an array can be regarded as a combination of two-hole structures. Here we propose a simpler method to treat the hole array.

As an example, we first consider a three-hole structure consisting of the open holes labeled by "1", "0" and "3" while other holes being closed in the array depicted in Fig. 1, referred to as 1-0-3 structure. In such a structure, if the transmissivity of the hole "0", denoted as T_{103} , is measured, one has to consider inter-hole effects between hole "0" and its two neighbors. Thus a reasonable expression should be

$$T_{103}(\theta) = T_0 + \Delta T_{01} + \Delta T_{03} = T_0 + T_{103}(\theta)C_{01} \sin^2 \theta + T_{103}(\theta)C_{03} \sin^2(\theta + 180^\circ) \quad (23)$$

Note that similar to the cases of 0-1 structure and 0-3 structures, the coefficients of the two interference terms should include a factor of the total transmissivity $T_{103}(\theta)$. Since the holes "1" and "3" are symmetric with respect to the hole "0", we have $C_{01} = C_{03}$. The difference of $T_{103}(\theta)$ between results of the calculation with Eq. (23) and simulation by FDTD method is about 1%.

From the example of the 1-0-3 structure it is concluded that for each additional hole, one merely simply add a term to embody the inter-hole effect, although the coefficient should be proportional to the total transmissivity of the hole "0". This conclusion can be extended into the whole array.

Now let the all holes in the array open. We calculate the transmissivity of hole "0". There are four nn and four nnn neighbors around this hole, labeled by "1" to "8", respectively. The

influence of the holes farther than the nnn ones is merged into the inter-hole effect between hole "0" and the eight neighbors, so that it needs not to consider. Thus, the transmissivity of hole "0" reads

$$T_{array} = T_0 + \sum_{i=1}^8 \Delta T_{0i}. \quad (24)$$

The second term in Eq. (24) includes the contribution from its all 8 neighboring holes.

When the hole array composes a square lattices with $A = B$.

First we study the case where all holes in the lattice are square, referred to as S-S array. The transmission in hole "0" is denoted as T_{S-S} .

The 0-1 and 0-5 structures have been studied in detail in Sec. 4. According to the conclusions of the two structures, we easily put down the terms of inter-hole effects contributed from all the eight neighboring holes as follows:

$$\Delta T_{01} = T_{S-S} C_{01} \sin^2 \theta, \quad (25a)$$

$$\Delta T_{02} = T_{S-S} C_{02} \sin^2(\theta - 90^\circ) = T_{S-S} C_{02} \cos^2 \theta, \quad (25b)$$

$$\Delta T_{03} = T_{S-S} C_{03} \sin^2(\theta - 180^\circ) = T_{S-S} C_{03} \sin^2 \theta, \quad (25c)$$

$$\Delta T_{04} = T_{S-S} C_{04} \sin^2(\theta - 270^\circ) = T_{S-S} C_{04} \cos^2 \theta, \quad (25d)$$

$$\Delta T_{05} = T_{S-S} C_{05} \sin^2(\theta + 45^\circ), \quad (26a)$$

$$\Delta T_{06} = T_{S-S} C_{06} \sin^2(\theta - 45^\circ), \quad (26b)$$

$$\Delta T_{07} = T_{S-S} C_{07} \sin^2(\theta - 135^\circ), \quad (26c)$$

$$\Delta T_{08} = T_{S-S} C_{08} \sin^2(\theta - 225^\circ). \quad (26d)$$

Here the azimuth of each neighboring hole is taken into account. Since the four holes "1" to "4" have the same distance away from "0", and the other four on the vertexes do so too, one naturally gets:

$$C_{01} = C_{02} = C_{03} = C_{04}, \quad (27a)$$

$$C_{05} = C_{06} = C_{07} = C_{08}. \quad (27b)$$

Inserting Eqs. (25)-(31) into (24), we obtain

$$T_{S-S} = T_0 + 2T_{S-S}(C_{01} + C_{05}) \quad (28)$$

Obviously, the transmission is independent of θ angle. This explains the experimental result of S-S array listed in Table 1.

If the parameters of the holes and lattice are the same as those in Sec. 4, we have $C_{01} + C_{05} = 0.103$, $T_0 = 19.35$, thus $T_{S-S} = 24.37$.

Next we study the case where the holes are square and the lattice is rectangular, referred to as S-R array. The transmission in hole "0" is denoted as T_{S-R} . Since in this case $B \neq A$, we define an angle α :

$$\alpha = \arctan(B/A). \quad (29)$$

The angular dependences of ΔT_{0i} , $i = 1, 2, 3, 4$ are the same as those in Eq. (25). One merely need to replace T_{S-S} in Eq. (25) by T_{S-R} to get the expression of ΔT_{0i} , $i = 1, 2, 3, 4$. However, since $B \neq A$, Eq. (27a) is not valid any more. We have following relationship:

$$C_{01} = C_{03} \neq C_{02} = C_{04}. \quad (30)$$

As for the neighbors "5" to "8", the angular dependence of interference terms are written as

$$\Delta T_{05} = T_{S-R} C_{05} \sin^2(\theta + \alpha), \quad (31a)$$

$$\Delta T_{06} = T_{S-R} C_{06} \sin^2(\theta - \alpha), \quad (31b)$$

$$\Delta T_{07} = T_{S-R} C_{07} \sin^2[\theta - (180^\circ - \alpha)] = T_{S-R} C_{07} \sin^2(\theta + \alpha), \quad (31c)$$

$$\Delta T_{08} = T_{S-R} C_{08} \sin^2[\theta - (180^\circ + \alpha)] = T_{S-R} C_{08} \sin^2(\theta - \alpha). \quad (31d)$$

The distance between the hole "0" and any one of these four holes is the same as others. Hence Eq. (27b) is still valid. Inserting Eqs. (30) and (31) into $T_{S-R} = T_0 + \sum_{i=1}^8 \Delta T_{0i}$, we have

$$T_{S-R} = T_0 + 2T_{S-R} \{ [C_{01} \sin^2 \theta + C_{02} \cos^2 \theta] + C_{05} [\sin^2(\theta - \alpha) + \sin^2(\theta + \alpha)] \}. \quad (32)$$

It is seen that the transmissivity of the S-T array depends on the polarization angle θ .

Thirdly we discuss the case where the holes are rectangular, $a \times b = 0.2 \times 0.1 \mu m^2$ and the lattice is square, $A = B = 0.4 \mu m$, the so-called R-S array. Since the transmission in each rectangular hole is dependent on θ , as manifested in Fig. 3(a), the single-hole effect is enough to cause the dependence of transmissivity T_{R-S} on the polarization angle. Besides, the inter-hole effect also influences T_{R-S} . Apparently, in this case we again have

relationship Eq. (30). In the case of $a \times b = 0.2 \times 0.1 \mu m^2$, the hole is regarded as a slit-hole, as having been mentioned in the last paragraph of Sec. 3 in explaining Fig. 4. Considering Eqs. (15) and (13), for a slit-hole, we have $\Delta S_{01,z}^{hole} = 2S_{01,z}^{hole} \gamma_{01} \sin^2 \theta = 0$, so $\Delta T_{01}(\theta) = T_{01}(\theta) C_{01}(\theta) \sin^2 \theta = 0$. Consequently $C_{01} = 0$. Following the method as above, the expression of the transmission is obtained as follows:

$$T_{R-S} = T_0(\theta) + 2T_{R-S}[C_{02}(\theta) \cos^2 \theta + 2C_{05}(\theta) \sin^2 45^\circ \cos^2 \theta],$$

By our simulation, it is approximately that $C_{02}(\theta) = 0.07/\cos^2 \theta$, $C_{05}(\theta) = 0.12/\cos^2 \theta$. Thus we get $T_{R-S} = 39.2 \cos^2 \theta$. The feature of T_{R-S} curve is the same as the experimental result [17]. This result confirms the validity of our calculation method.

Finally, for the case of a rectangular lattice comprising rectangle holes, R-R array, we can use the same method to discuss the transmission T_{R-R} . But we do not put down the formula. A qualitative conclusion is obvious. Since both the single holes and lattice are rectangular, it is sure that T_{R-R} depends on the polarization angle.

6. Applications

Up to now we have discussed the six cases in Table 1. The two kinds of single holes are studied in detail in Sec. 3 and the four kinds of arrays are investigated in Sec. 5. The mechanism of the polarization dependence of the transmission of each case is explicitly disclosed. A simple method is proposed to evaluate the transmissivity of the arrays. The physical meaning of this method is that it exhibits the transmission is mainly from two parts: the single-hole and inter-hole effects. The obvious advantage of this method is that it reduces the workload greatly compared to the simulation of the whole array.

Among four kinds of arrays in Table 1, two, S-S and R-S arrays, have been investigated experimentally, while the other two, S-R and R-R arrays, have not. Here we employ our method to calculate the transmissivity T_{S-R} and T_{R-R} of S-R and R-R arrays. The numerical results are provided for someone to test.

For an S-R array, we chose $A = 0.4 \mu m$, $B = 0.3 \mu m$, and $a \times b = 0.2 \times 0.2 \mu m^2$. In this structure, $C_{01} = 0.255$ is unchanged, and C_{02} and C_{05} have to be estimated. The transmissivities of 0-2 and 0-5 structures are simulated and fitted by $T_{02} = T_0 + 0.12T_{02} \cos^2 \theta$ and $T_{05} = T_0 - 0.08T_{05} \sin^2[\theta - \arctan(0.3/0.4)]$, so we get $C_{02} = 0.12$ and $C_{05} = -0.08$.

Then the transmissivity is expressed by

$$T_{S-R} = 19.36 / \{1 - 2(0.255 \sin^2 \theta + 0.12 \sin^2 \theta) + 2 \times 0.08[\sin^2(\theta - 36.9^\circ) + \sin^2(\theta + 36.9^\circ)]\}$$

The calculated curve is displayed in Fig. 7(a).

For an R-R array, we take $A = 0.4\mu m$, $B = 0.3\mu m$ and $a = 0.2\mu m$, $b = 0.1\mu m$. For such a slit-hole, $C_{01} = 0$. In 0-2 and 0-5 structures, the simulation results are $T_{02} = T_0(\theta) + 6 \cos^2 \theta$ and $T_{05} = T_0(\theta) + 6.1 \sin^2(36.9^\circ) \cos^2 \theta$ respectively. Here $T_0(\theta)$ is the single hole transmissivity expressed in Fig. 3(a) with the formula $T_0(\theta) = 24.3 \cos^2 \theta$. When writing formulas in the coupling form, $T_{02} = T_0(\theta) + C_{02} T_{02} \cos^2 \theta$ and $T_{05} = T_0(\theta) + C_{05} T_{05} \sin^2(36.9^\circ) \cos^2 \theta$, we obtain $C_{02}(\theta) = 0.2 / \cos^2 \theta$ and $C_{05}(\theta) = 0.023 / \cos^2 \theta$. It is found that C_{02} and C_{05} vary with θ and cannot be regarded as constants now. This arises from that $T_0(\theta)$ varies with θ in this structure. Equation (27b) still holds in this lattice. $C_{06}(\theta) = 0.023 / \cos^2 \theta = C_{07}(\theta) = C_{08}(\theta)$. Thus the coupling equation is $T_{R-R} = T_0(\theta) + 2T_{R-R}[C_{02}(\theta) \cos^2 \theta + 2C_{05}(\theta) \sin^2(36.9^\circ) \cos^2 \theta]$. The calculated T_{R-R} is plotted in Fig. 7(b). Comparing Fig. 7(a) and (b), we see that the variation scope of T_{R-R} is larger than that of T_{S-R} , since the R-R array has a stronger anisotropy than S-R array. Especially, T_{R-R} can be zero at $\theta = 90^\circ$.

7. Summary

We have investigated the polarization dependences of the transmission in square and rectangular lattices consisting of different subwavelength holes. The field components and transmissivities of single-hole and double-hole structures are computed by use of FDTD simulation method. The behaviors of the transmission are explored and the corresponding mechanisms are disclosed. Our basic point of view is that the total transmissivity of a hole array is determined by the two basic factors: the single-hole effect and inter-hole effects. Based on the results of these structure, a compact method is suggested and applied to investigate the hole arrays. Our conclusions are summarized as follows. (1) The SPP PERs are key roles in single hole. In a square hole the SPP PERs along the two sides of the hole are equal, which leads to two consequences. One is that the SPP wave in the square hole is along the polarization direction of the incident light, and the other is that the amplitude of the SPP wave is in proportion to that of the incident light at any polarization angle. By contrast, in a rectangle hole, the SPP PERs is not isotropic, which results in that the amplitude of SPP

in a rectangle hole cannot reserve a fixed proportion to that of incident light with different polarization angle. Therefore the transmissivity depends on the polarization angle. (2) The transverse magnetic field of the SPP wave on the metal film surface plays a key role in the inter-hole effect. (3) The total transmissivity of the hole array can be expressed with the single-hole transmissivity plus the terms reflecting inter-hole effects between the hole and its nn and nnn neighbors. (4) The conclusion (3) provides a simple method to calculate the transmissivity of the hole arrays. By this method we calculated the polarization dependence of the transmissivity for S-R and S-S arrays that are not reported in literatures.

Acknowledgements

This work is supported by the 973 Program of China (Grant No.2011CB301801) and the National Natural Science Foundation of China (Grant No. 10874124), and Natural Science Foundation of Beijing (No. 1102012).

† E-mail: 263zys@263.net

‡ E-mail: wanghuaiyu@mail.tsinghua.edu.cn

Reference

- [1] Ebbesen T W, Lezec H J, Ghaemi H F *et al* 1998 Extraordinary optical transmission through sub-wavelength hole arrays *Nature* **391** 667
- [2] Lezec H J, Degiron A, Devaux E *et al* 2002 Beaming light from a subwavelength aperture *Science* **297** 820
- [3] Altewischer E, van Exter M P and Woerdman J P *et al* 2002 Plasmon-assisted transmission of entangled photons *Nature* **418** 304
- [4] Altewischer E, Genet C, van Exter M P *et al* 2005 Polarization tomography of metallic nanohole arrays *Optics Letters* **30** 1
- [5] Gordon R, Brolo A G, McKinnon A *et al* 2004 Strong polarization in the optical transmission through elliptical nanohole arrays *Phys.Rev.Lett.* **92** 037401
- [6] Altewischer E, van Exter M P and Woerdman J P 2003 Polarization analysis of propagating surface plasmons in a subwavelength hole array *J. Opt. Soc. Am. B* **20** 1927
- [7] Genet C, Altewischer E, van Exter M P *et al* 2005 Optical depolarization induced by arrays

- of subwavelength metal holes *Phys.Rev.B* **71** 033409
- [8] Sarrazin M and Vigneron J P 2004 Polarization effects in metallic films perforated with a bidimensional array of subwavelength rectangular holes *Optics Communications* **240** 89
- [9] Yanik A A, Wang X, Erramilli S *et al* 2008 Mid-Infrared subwavelength polarization optics with plasmonic nanostructures *Lasers and Electro-optics society, LEOS 2008 The 21st Annual Meeting of the IEEE* 490 - 491
- [10] Roth R M, Panoiu N C, Adams M *et al* 2006 Polarization-sensitive extraordinary transmission through periodic arrays of crossed nano-slits mediated by local surface plasmons *Conference Paper OSA/NANO, NFA4*
- [11] Lee J W, Seo M A, Park D *et al* 2006 Shape resonance omni-directional terahertz filters with near-unity transmittance *Optics Express* **14** 3
- [12] Zhao G Z, Wang Y, Zhang C *et al* 2007 Polarization dependence of transmission of terahertz radiation through periodic array of subwavelength rectangular holes *IEEE:IRMMW-THz'2007* pp821-822
- [13] Ren X F, Guo G P, Huang Y *et al* 2007 Influence of unsymmetrical periodicity on extraordinary transmission through periodic arrays of subwavelength holes *Appl. Phys. Lett.* **90** 161112
- [14] Degiron A, Lezec H J, Yamamoto N, *et al* 2004 Optical transmission properties of a single subwavelength aperture in a real metal *Optics Communications* **239** 61
- [15] Degiron A and Ebbesen T W 2005 The role of localized surface plasmon modes in the enhanced transmission of periodic subwavelength apertures *J.Opt.A* **7** S90
- [16] Ren X F, Zhang P, Guo G P *et al* 2008 Polarization properties of subwavelength hole arrays consisting of rectangular holes *Appl. Phys.B* **91** 601
- [17] Jeffrey R DiMaio and John Ballato 2006 Polarization-dependent transmission through subwavelength anisotropic aperture arrays *Optics.Express* **14** 6
- [18] Hu D and Zhang Y *et al* 2009 Surface plasmons based transmission enhancement of terahertz through metal aperture arrays *SPIE* **73850** Z-1
- [19] Hu D and Zhang Y *et al* 2010 Localized surface plasmons-based transmission enhancement of terahertz radiation through metal aperture arrays *Optik* **121** 1423
- [20] The theoretical works are reviewed by Konstantin Y. Bliokh *et al* 2008 Unusual resonators: Plasmonics, metamaterials, and random media *Reviews of Modern Physics* **80** 1201.

- [21] Garcia de Abajo F. J. *et al* 2005 Full transmission through perfect-conductor subwavelength hole arrays *Phys. Rev. E* **72**, 016608.
- [22] Gordon R., *et al*, 2004 Strong Polarization in the Optical Transmission through Elliptical Nanohole Arrays *Phys. Rev. Lett.* **92**, 037401.
- [23] Gomez-Medina R. *et al* 2006, Extraordinary optical reflection from sub-wavelength cylinder arrays, *Opt. Express* **14**, 3730.
- [24] Elliott, J. *et al* 2004, Polarization control of optical transmission of a periodic array of elliptical nanoholes in a metal film *Opt. Lett.* **29**, 1414.
- [25] Martin-Moreno, L. *et al*, 2001, Theory of extraordinary optical transmission through subwavelength hole arrays *Phys. Rev. Lett.* **86** 1114.
- [26] Zhou Y S, Gu B Y, Lan S *et al* 2008 Time-domain analysis of mechanism of plasmon-assisted extraordinary transmission *Phys. Rev. B* **78** 081404(R)
- [27] The commercially available software developed by Rsoft Design Group <http://www.rsoftdesign.com> is used for the numerical simulations.
- [28] Zhou Y S, Gu B Y, Wang H Y *et al* 2009 Multi-reflection process of extraordinary optical transmission in a single subwavelength metal slit *Europhysics Lett.* **85** 24005

Figure captions

Fig.1 The sketch of a metal hole array consisting of subwavelength rectangle holes.

Fig.2 The simulated transmissivity T_0 and polarization dependence of amplitudes of the electric and magnetic fields in a single-square-hole structure. The fitting curves are calculated by Eq. (3).

Fig.3 The polarization dependence of quantities for a rectangle hole. (a) The transmissivity. The fitting curve is $T_0(\theta) = 24.3 \cos^2 \theta$. (b) The amplitudes of the electric and magnetic fields. The fitting curves are calculated by Eq. (3).

Fig.4 The SPP polarization excitation rations of a rectangle hole with $a = 0.2\mu m$ and b varies from 0.1 to $0.3\mu m$. The lines are just to guide eyes.

Fig.5 (a) The polarization dependence of the transmissivity T_{01} for a two-hole structure. The fitting solid curve is from Eqs. (10) and (11). The dashed curve is obtain by the approximation of $C_{01} = 0.255$. (b) The amplitudes of the electric and magnetic fields along the metal surface yielded from a single hole. The fitting curves are from Eq. (12).

Fig.6 The simulated transmissivity in a 0-5 structure. The dashed curve is plotted by the fitted formula in the approximation of $C_{05} = -0.152$.

Fig.7 The calculated transmissivity in (a) the S-R array and (b) The R-R array.

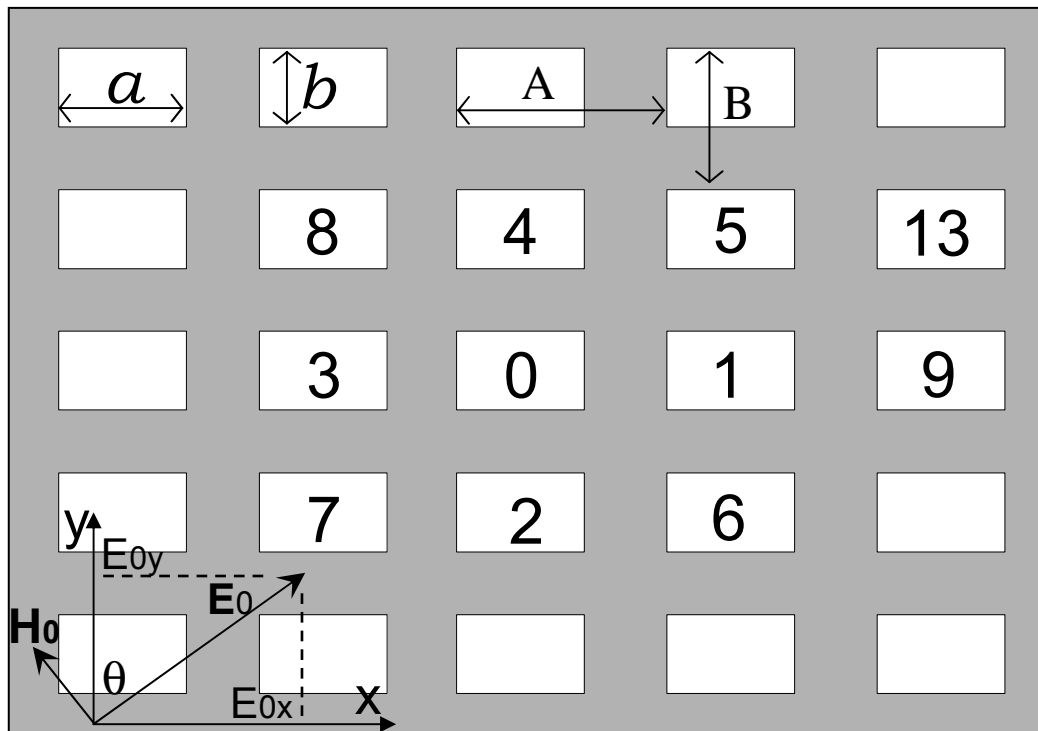


Fig. 1 (Zhao et al)

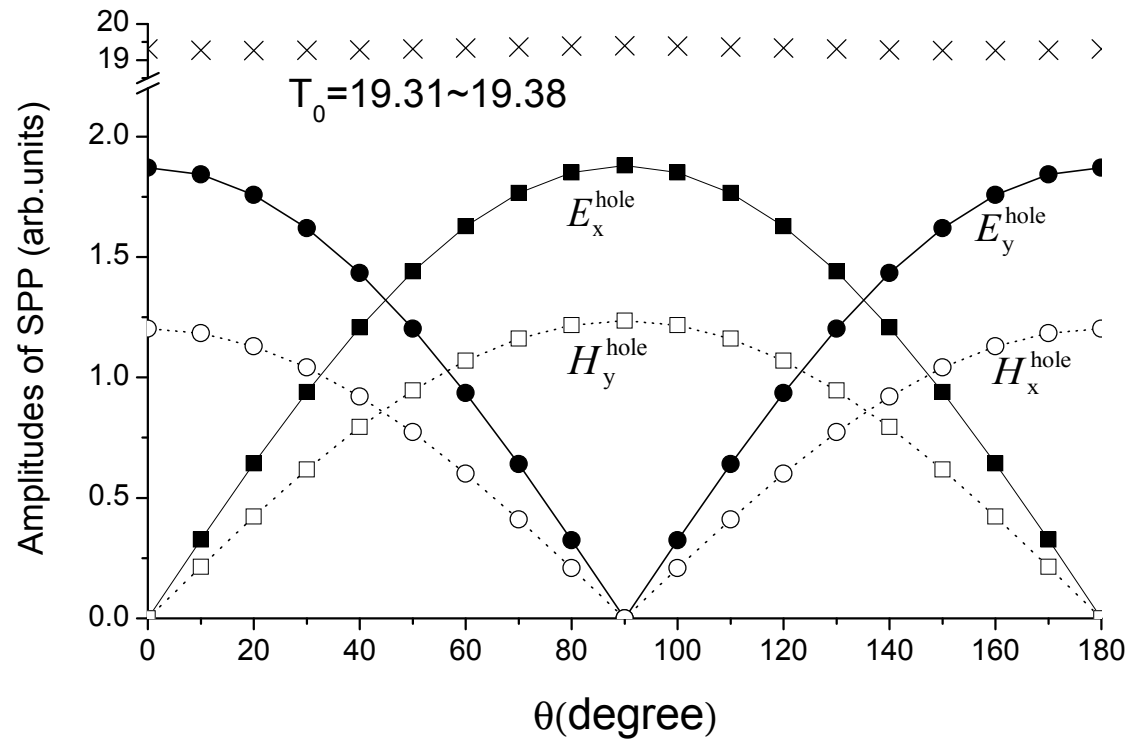


Fig. 2 (Zhao et al)

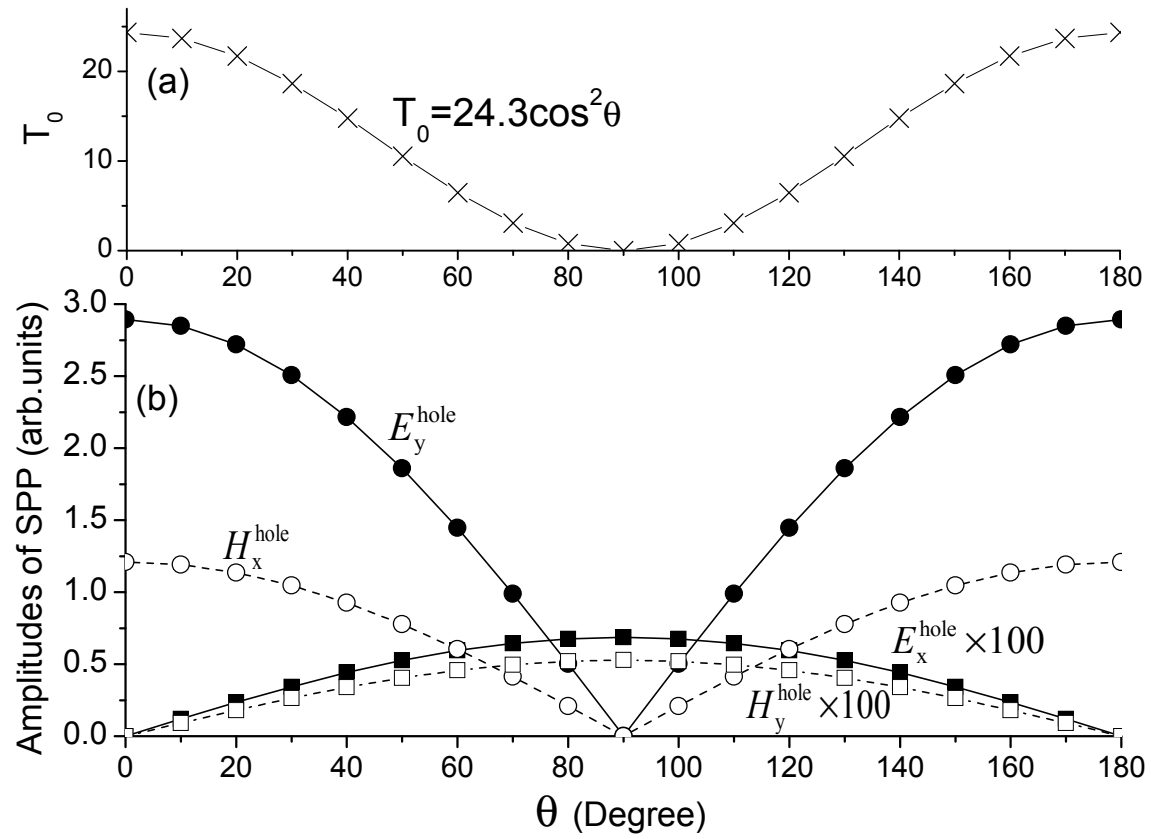


Fig.3 (Zhao et al)

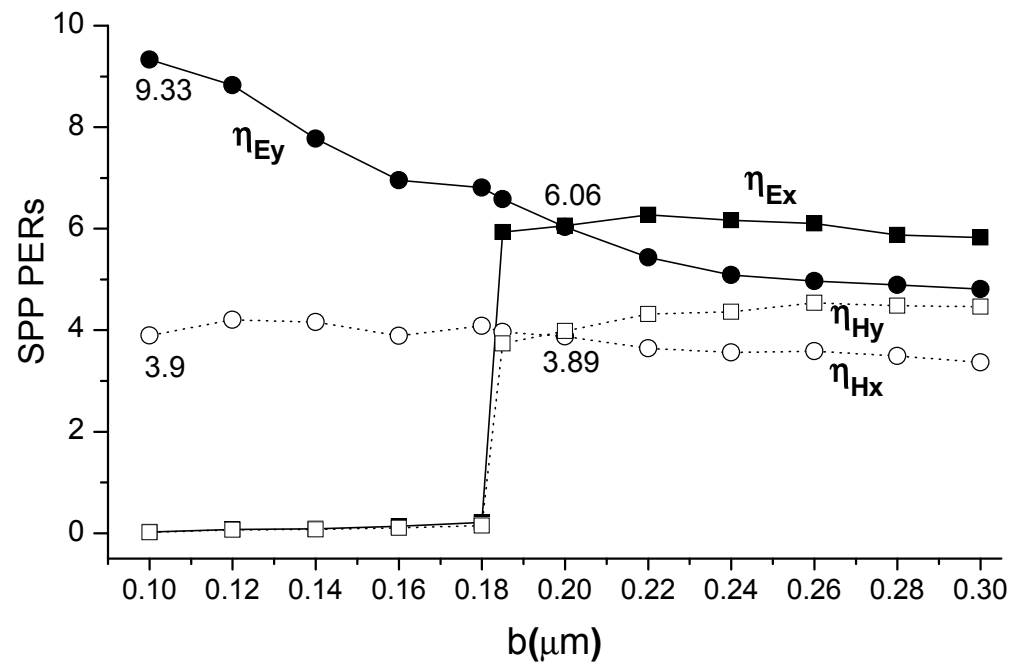


Fig.4 (Zhao et al)

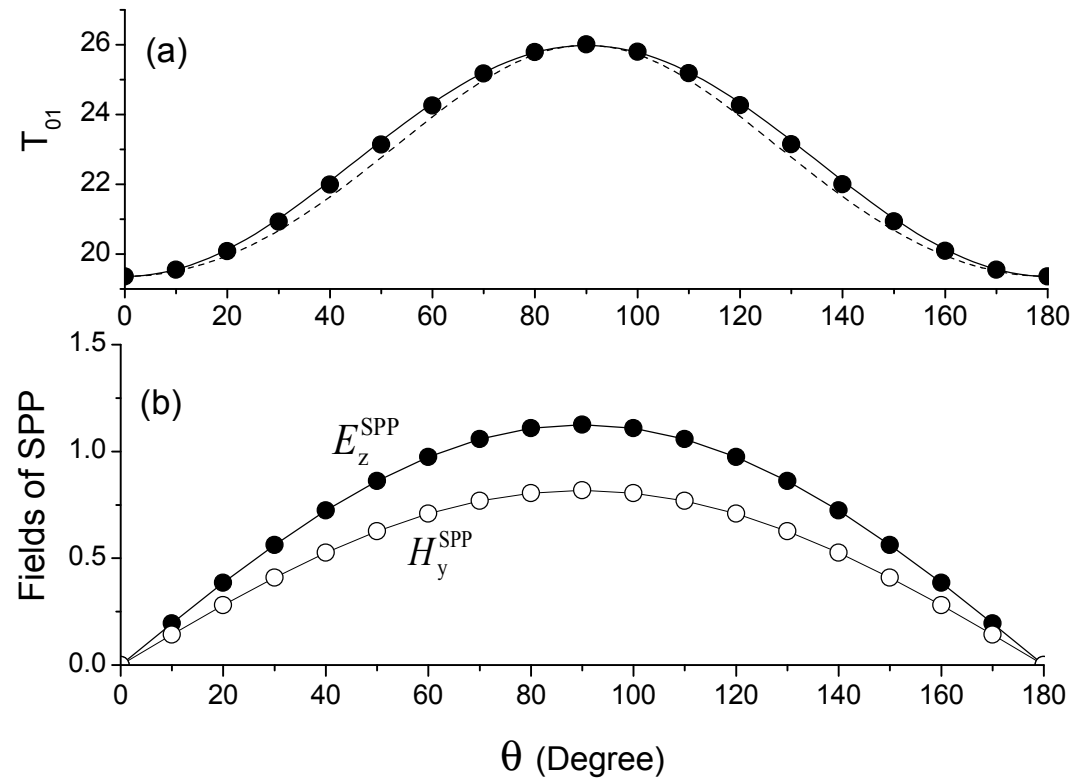


Fig.5 (Zhao et al)

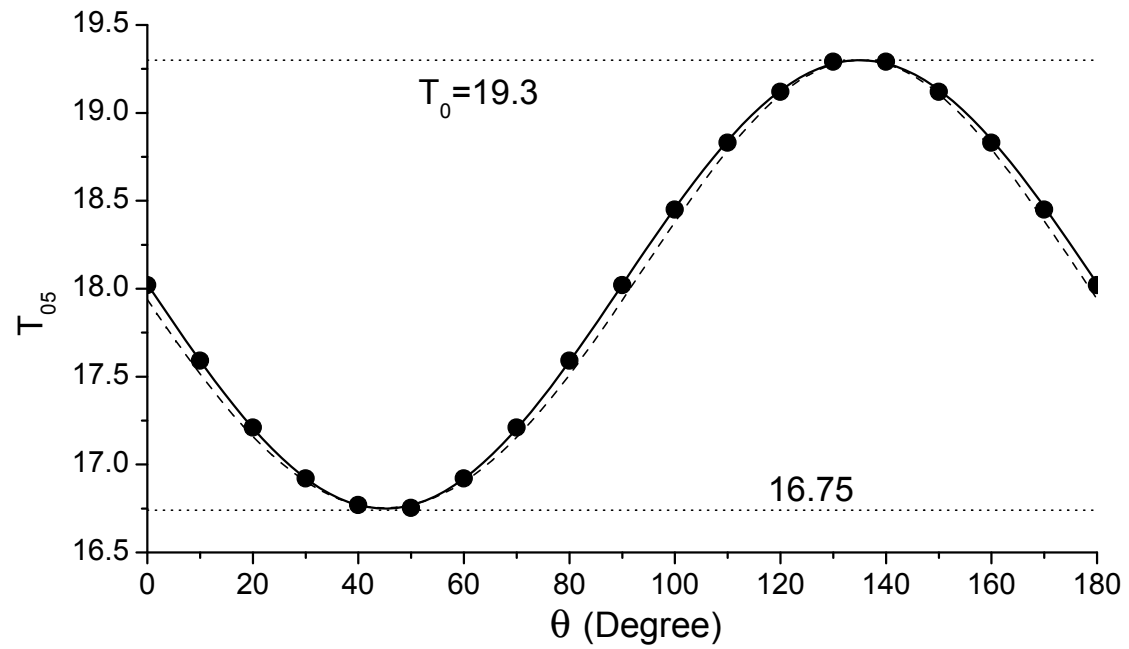


Fig.6 (Zhao et al)

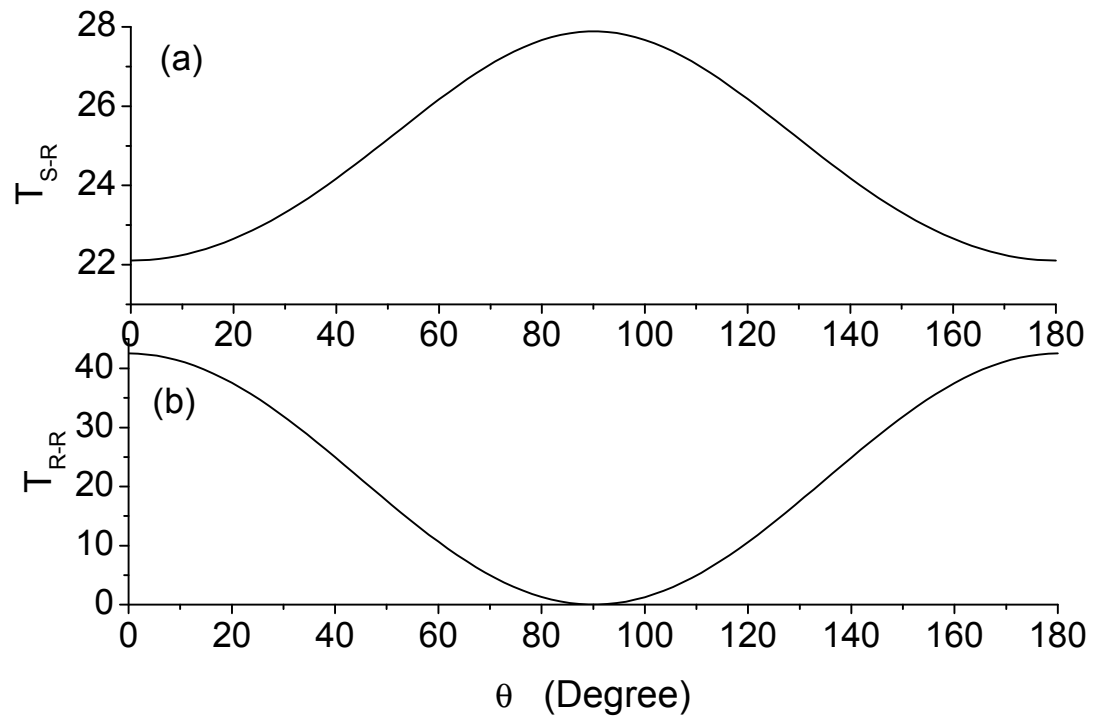


Fig. 7 (Zhao et al)